

Modeling of Surface Plasmon Mode of Gold Nanoslit-based Biosensor

Jui-Teng Lin¹ Hsia-Wei Liu²

¹ New Vision Inc,
Taipei 10476, Taiwan, ROC
jtlin55@gmail.com

² Department of Life Science, Fu Jen Catholic University,
New Taipei City 24205, Taiwan, ROC
079336@mail.fju.edu.tw

Received 10 May 2013; Revised 28 August 2013; Accepted 16 September 2013

Abstract. The nonlinear optical features of surface plasmon resonance (SPR) wave propagating along the metallic interface (SPR-mode) of a nanoslit array are presented. The SPR resonance wavelength is decided by the nanoslit period (P) and the refractive index (RI) of the sensing medium (n). Approximate analytic formulas and fit equations are derived and compared with the exact numerical results. The real part of gold dielectric function is fit to a quadratic equation which covers wider range of the SPR resonance wavelength (600-4000 nm) than the prior linear fit (600-1000 nm). A nonlinear fit RI sensitivity (M) is found to be $M = P + 7.46n$ which is much more accurate than the first order approximation, $M=P$. The figure of merit defined by the ratio of M and the spectrum broadening is also calculated and showing an optimal period.

Keywords: biosensor, nanoslit, surface plasma resonance, nanogold, sensitivity

1 Introduction

The extraordinary transmission of a TM wave in nanoslits has been observed, in which there are two types of resonance waves: the surface plasmon resonance (SPR) wave propagating along the metallic interface (SPR-mode) and the gap resonance wave inside the nanoslit cavity (cavity mode) [1–15]. Comparing to the nanoholes array with a cutoff frequency limitation [9], nanoslits provide not only higher sensitivity but also much wider resonance spectrum [8]. This paper will focus on the SPR mode and the nonlinear feature of its resonance wavelength and the associate refractive index (RI) sensitivity as a function of the period and sensing medium RI. Approximate analytic formulas and fit equations will be derived and compare with the exact numerical results. The figure of merit defined by the ratio of the sensitivity and the spectrum broadening is also calculated showing an optimal slit period. Finally the role of silica layer (coated on top of the gold metallic array) is studied by an effective refractive index. The measured data of the sensitivity and further resonance wavelength red-shift due to the silica film are analyzed. The explicit formulas presented in this article provide useful guidance for SPR mode in gold nanoslit, particularly for the nonlinear features which have not been explored experimentally or theoretically.

2 Theory

The device to be analyzed is shown in Fig. 1, where the nanoslits array is defined by the period P , grooves width d , and metal (gold) height h . On top of the gold nanoarray, silica layer with a thickness t is coated. In general, there are two types of resonances: the surface plasmon resonance on the gold-silica-medium interface (SPR-mode) and the gap-resonance inside the slit (cavity-mode). The cavity-mode is characterized by the effective refractive index inside the slit (N_{eff}), the width (d) and height (h) of the slits, the period (P) and the resonance wavelength (λ), given by the phase matching condition [12,13].

$$h = \frac{\lambda}{4\pi N_{eff}} (2q\pi + \phi_1 + \phi_2) \quad (1)$$

where $q = 1, 2, \dots$ is the mode number and ϕ_j ($j = 1, 2$) are the phase shift at the top and bottom interface. Due to the complex nonlinear behavior of N_{eff} and the phase-shift factor, the resonance wavelength condition of Eq. (1)

would need numerical simulations which will be presented elsewhere. This paper will focus on the nonlinear features of the SPR modes and the influence of the silica coating.

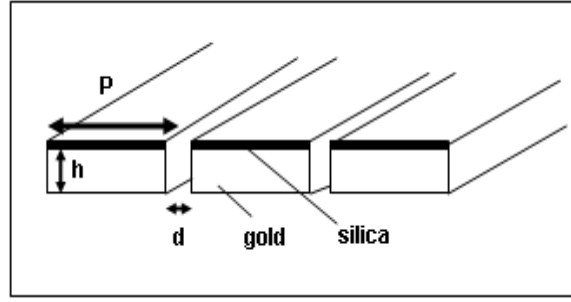


Fig. 1. Schematic of a nanoslits array defined by the period P , grooves width d , and metal (gold) height h . On top of the gold array, silica layer with a thickness t is coated.

2.1 Exact Formulas for SPR-mode

We will first study the case that there is no silica film or the silica film thickness is much smaller than that of gold; therefore the RI of the silica plays no roles. An effective RI will be introduced later to include the influence of the silica film. The SPR-mode of the gold-only nanoslits has a resonance wavelength given by the resonance condition [1,12,13].

$$\lambda = \frac{nP}{\sqrt{1 + n^2 / \varepsilon(\lambda)}} \quad (2)$$

where n is the refractive index (RI) of the sensing medium, and $\varepsilon(\lambda)$ is the real part of gold dielectric function, reported by Johnson and Christy, which may be fit to a linear [16,17], for short wavelength range (600-1000 nm) or nonlinear equation (for all range) as follows,

$$\varepsilon(\lambda) = 33 - 0.071\lambda \quad (3.a)$$

$$\varepsilon(\lambda) = 12.5 - 0.02\lambda - 0.0000333\lambda^2 \quad (3.b)$$

Eq. (2) is highly nonlinear due to the wavelength-dependence of $\varepsilon(\lambda)$ and cannot be solved analytically for the P and n dependence of the resonance wavelength. Therefore a converted formula is derived from Eq. (2)

$$P = (\lambda/n) \sqrt{1 + \frac{n^2}{\varepsilon(\lambda)}} \quad (4)$$

which gives the explicit form of P as function of the resonance wavelength and medium RI (n). Above equation allows us to plot P versus λ for a given $n = 1.0$ (in air) or 1.33 (in water). The 90-degree angle rotated-axis plot gives us λ versus P , which may be fit to an analytic express of λ as function of P and n (to see shown later).

Another useful explicit formula is also derived from Eq. (2) as follows:

$$n = \frac{\lambda}{P} \sqrt{1 - \frac{(\lambda/P)^2}{\varepsilon(\lambda)}} \quad (5)$$

Similar to the case for λ versus P , one may plot the rotated-axis showing λ versus n , and its slope give us the sensitivity function defined by $M = d\lambda/dn$ at a given P .

2.2 Approximate Formulas

Analytic expression for the resonance wavelength given by Eq. (2) may be derived by the using the first-order approximation $\lambda = nP$ in Eq. (3) $\varepsilon \approx 33.05 - 0.071(nP)$ to obtain

$$\lambda \approx (nP) \sqrt{1 + \frac{14.08n}{P[1 - 465/(nP)]}} \quad (6)$$

Therefore the approximate sensitivity function $M = d\lambda/dn$ is given by

$$M \approx P + 14.08n + \frac{3274}{P} \quad (7)$$

which shows that the nonlinear term of Eq. (6) results its slope function (M) depending on the sensing medium RI (n) and the period (P). Therefore Eq. (6) and (7) are better approximation than the first-order relation of $M = P$ which is independent to n .

3 Results and discussion

3.1 Application Wavelength Range

As shown in Fig. 2, the linear fit of Eq. (3.a) for the real part of gold dielectric function is only good for short wavelength range of 600-1200 nm and suffers huge errors for long wavelength (>1500 nm). For biosensor nanoarray applications with typical range of $P = (600 - 900)$ nm and the associate resonance wavelength of (in water medium) in the near infrared 800-1,200 nm, either linear or nonlinear fit equation may be used. However, for other photonic applications such as telecommunication, wave guided resonator and grating filter using microarray with period $P > 1.5$ microns the nonlinear fit equation is required.

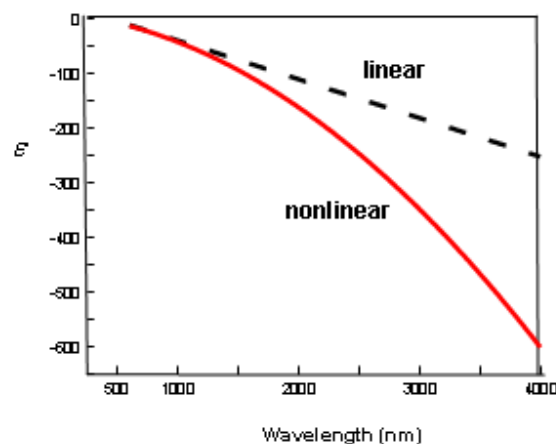


Fig. 2. Real parts of gold dielectric function as function of wavelength. Dashed curve is based on the linear fit Eq. (3.a) and solid curve is the nonlinear fit Eq. (3.b).

3.2 Exact versus Approximate Calculations

Fig. 3 shows the period P is an increasing function of the resonance wavelength based on the exact expression of Eq. (4). It also shows that for a given P , the resonance wavelength is red-shifted when the sensing medium RI increases. To include the P dependence of the resonance wavelength, we obtain the alternative equation fit to both Fig. 3. as follows:

$$\lambda(P, n) = (P - 15.31)n + 10.17n^2 + 18099 / P \quad (8.a)$$

and the slope function

$$M = P - 15.31 + 20.34n \quad (8.b)$$

We note that the above numerically-fit equations Eq (10) is more accurate than the analytic approximate Eq. (6) and (7). The P dependence of M is plot in Figure 6 showing that the nonlinear-fit Eq. (8) matches very well with the exact curve but the first order approximation given by $M = P$ is undervalued 14.9 nm/RIU in water medium. Our calculated exact resonance wavelength 825 nm (for $P = 600$ nm in water medium) is close to the measured value 807 nm of Lee et al [15] and our calculated sensitivity, based on Eq. (9), $M = 615.4$ nm/RIU, is about 10% lower than their measured data 689 nm/RIU.

3.3 The Figure of Merit

The figure of merit (FOM) of the nanoslit sensor is defined by the ratio of the RI sensitivity (M) and the full-width-at half maximum (FWHM) of the gold spectrum broadening. Using the FWHM of solid-gold nanoparticles, shown by Figure 4 and M shown by Eq. (9), we show the FOM= M /FWHM in Figure 5 as a function of P . It should be noted that an optimal P is around 500 nm, or the associate resonance wavelength of (700-750) nm depending on the RI of the sensing medium given by an approximated fit equation $\lambda = (P + 3.73n) n$.

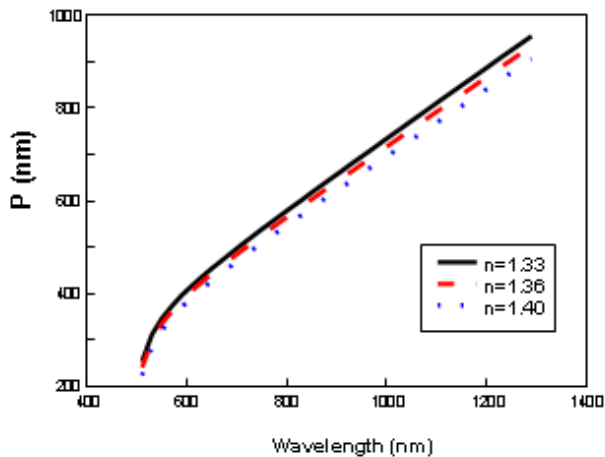


Fig. 3. Nanoslit period P as a function of the SPR mode resonance wavelength at various medium refractive indexes (n) based on the exact numerical solution of Eq. (4).

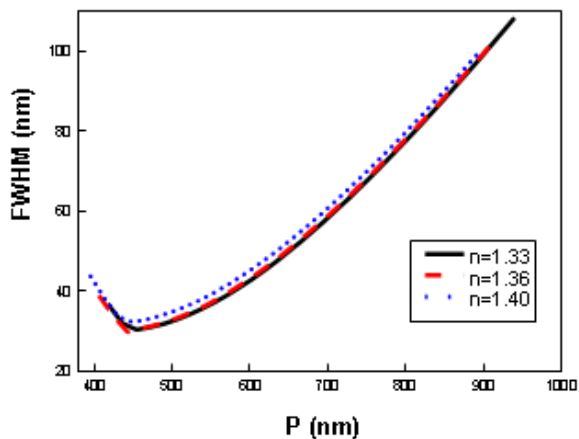


Fig. 4. Full-width-at-half maximum (FWHM) of nanogold spectrum broadening versus period (P) for various sensing medium RI (n).

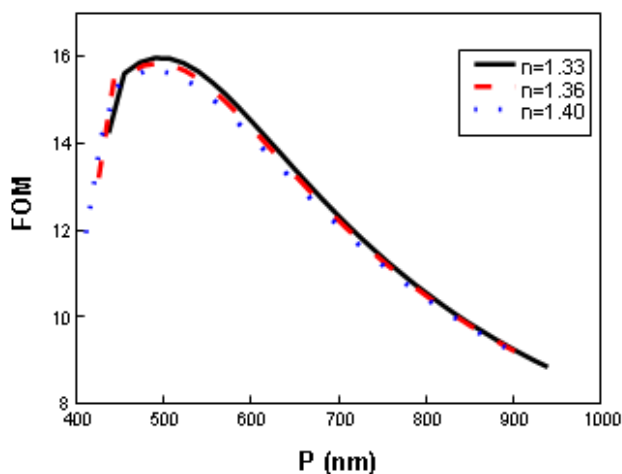


Fig. 5. Figure of merit (FOM) of the nanoslit sensor defined by $M/FWHM$ associate to Fig. 4 [13].

4 Conclusion

We have showed that the real part of gold dielectric function fit to a quadratic equation covers wider range of the SPR resonance wavelength (600–4000 nm) than the prior linear fit (600–1000 nm). A nonlinear fit RI sensitivity (M) is also more accurate than the first order approximation, $M=P$, and showing the P and n dependence. The figure of merit defined by the ratio of M/FWHM shows an optimal period about $P = 500$ nm. Finally, the roles of silica layer thickness may be calculated from an effective refractive index and a reduced thickness. The measured data of the sensitivity and further resonance wavelength red-shift due to the silica film are consistent with our calculations. The explicit formulas presented in this article provide useful guidance for SPR mode in gold nanoslit, particularly for the nonlinear features which have not been explored experimentally or theoretically.

Acknowledgement

This work is partially supported by the National Science Council (NSC) of Taiwan, R.O.C. (grant No. NSC 100-2221-E-030-001). It is also partially supported by the grant from Xiamen-200 program (Xiamen Science & Technology Bureau, China). The authors thank the assistance from Yu-Ling Hong for numerical drawings.

References

- [1] T. W. Ebbesen, H. J. Lezec, H. F. Ghaemi, T. Thio, P. A. Wolff, "Extraordinary Optical Transmission through Sub-Wavelength Hole Arrays," *Nature*, Vol. 391, pp. 667–669, 1998.
- [2] M. Skorobogatiy and A. V. Kabashin, "Photon Crystal Waveguide-Based Surface Plasmon Resonance Biosensor," *Appl. Phys. Letter*, Vol. 89, pp. 143518, 2006.
- [3] H. Caglayan and E. Ozbay, "Surface Wave Splitter Based on Metallic Gratings with Sub-wavelength Aperture," *Opt. Express*, Vol. 16, pp. 19091–19096, 2008.
- [4] P. Lalanne, J.P. Hugonin, J.C. Rodier, "Theory of Surface Plasmon Generation at Nanoslit Apertures," *Phys. Rev. Letter*, Vol. 95, No. 26, 2005.
- [5] Y. S. Jung, Y. Xi, J. Wuenschell, H.K. Kim, "Near-to far-field Imaging of Phase Evolution of Light Emanating from a Metal Nanoslit," *Opt. Express*, Vol.16, pp. 18881–18882, 2008.
- [6] B. Wang and P. Lalanne, "How Many Surface Plasmons Are Locally Excited on the Ridges of Metallic Lamellar Gratings," *Appl. Phys. Letter*, Vol. 96, pp. 051115–051113, 2010.
- [7] S. I. Bozhevolnyi, J. Erland, K. Leosson, P. M.W. Skovgaard, J. M. Hvam, "Waveguiding in Surface Plasmon Polariton Band Gap Structures," *Phys. Rev. Letter*, Vol. 86, pp. 3008–3011, 2001.
- [8] Holmgaard and S. I. Bozhevolnyi, "Theoretical Analysis of Dielectric-Loaded Surface Plasmon-Polariton Waveguides," *Phys. Rev. B*, Vol. 75, pp. 245405, 2007.
- [9] A. G. Brolo, R. Gordon, B. Leathem, K. L. Kavanagh, "Surface Plasmon Sensor Based on the Enhanced Light Transmission Through Arrays of Nanoholes in Gold Films," *Langmuir*, Vol. 20, pp. 4813–4815, 2004.
- [10] R. Gordon, "Near-field Interference in a Subwavelength Double Slit in a Perfect Conductor," *J. Opt. A: Pure Appl. Opt.*, Vol. 8, pp. L1–L3, 2006.
- [11] H. Shi, X. Luo, C. Du, "Young's Interference of Double Metallic Nanoslit With Different Widths," *Opt. Express*, Vol. 15, pp. 11321–11327, 2007.
- [12] H. Raether, *Surface Plasmons on Smooth and Rough Surfaces and On Gratings*, Springer Verlag, Berlin, 1988.

- [13] P. Lalanne, C. Sauvan, J. P. Hugonin, J. C. Rodier, P. Chavel, "Perturbative Approach for Surface Plasmon Effects on Flat Interfaces Periodically Corrugated by Subwavelength Apertures," *Phys. Rev. B*, Vol. 68, p. 125404, 2003.
- [14] K. L. Lee, C. W. Lee, W. S. Wang, P. K. Wei, "Sensitive Biosensor Array Using Surface Plasmon Resonance on Metallic Nanoslits," *J Biomed Optics*, Vol. 12, pp. 044023, 2007.
- [15] K. L. Lee, W. S. Wang, P. K. Wei, "Sensitive Label-Free Biosensors By Using Gap Plasmons in Gold Nanoslits," *Biosen and Bioelectron*, Vol. 24, pp. 210–215, 2008.
- [16] B. Yan, Yang, Y. and Wang, Y., "Comment on: Simulation of the Optical Absorption Spectra of Gold Nanorods as a Function of Their Aspect Ratio and the Effect of the Medium Dielectric Constant," *J. Phys. Chem. B.*, Vol. 107, pp. 9159– 9159, 2003.
- [17] S. Link and El-Sayed, M.A., "Simulation of the Optical Absorption Spectra of Gold Nanorods as a Function of Their Aspect Ratio and the Effect of the Medium Dielectric Constant," *J. Phys. Chem. B.*, Vol. 109, pp. 10531–10532, 2005.